ACCOUNTS
of chemical research

Nanoparticulate X-ray Computed Tomography Contrast Agents: From Design Validation to in Vivo Applications

YANLAN LIU,[†,‡] KELONG AI,[†] AND LEHUI LU*[,†]

[†]*State Key Laboratory of Electroanalytical Chemistry, Changchun Institute of Applied Chemistry, Chinese Academy of Sciences, Changchun 130022, P. R. China, and* [‡]*Graduate School, Chinese Academy of Sciences, Beijing 100039, P. R. China*

RECEIVED ON MAY 19, 2012

CONSPECTUS

X-ray computed tomography (CT) is one of the most powerful noninvasive diagnostic imaging techniques in modern medicine. Nevertheless, the iodinated molecules used as CT contrast agents in the clinic have relatively short circulation times in vivo, which significantly restrict the applications of this technique in target-specific imaging and angiography. In addition, the use of these agents can present adverse. For example, an adult patient typically receives approximately 70 mL of iodinated agent (350 mg I/mL) because of iodine's low contrast efficacy. Rapid renal clearance of such a large dose of these agents may lead to serious adverse effects. Furthermore, some patients are hypersensitive to iodine.

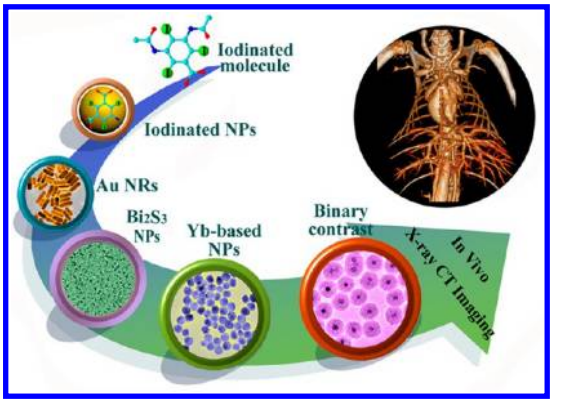

Therefore, biomedical researchers have invested tremendous efforts to address these issues. Over the past decade, advances in nanoscience have created new paradigms for imaging. The unique properties of nanomaterials, such as their prolonged circulating half-life, passive accumulation at the tumor sites, facile surface modification, and integration of multiple diverse functions into a single particle, make them advantageous for in vivo applications. However, research on the utilization of nanomaterials for CT imaging has lagged far behind their applications for other imaging techniques such as MRI and fluorescence imaging because of the challenges in the preparation of cost-effective nanoparticulate CT contrast agents with excellent biocompatibility, high contrast efficacy, long in vivo circulation time, and long-term colloidal stability in physiological environments.

This Account reviews our recent work on the design and in vivo applications of nanoparticulate CT contrast agents. By optimizing the contrast elements in the nanoparticles according to the fundamental principles of X-ray imaging and by employing the surface engineering approaches that we and others have developed, we have synthesized several nanoparticulate CT contrast agents with excellent imaging performance. For example, a novel Yb-based nanoparticulate agent provides enhanced contrast efficacy compared to currently available CT contrast agents under normal operating conditions. To deal with special situations, we integrated both Ba and Yb with great differential in K-edge value into a single particle to yield the first example of binary contrast agents. This agent displays much higher contrast than iodinated agents at different voltages and is highly suited to diagnostic imaging of various patients. Because of their prolonged in vivo circulation time and extremely low toxicity, these agents can be used for angiography.

1. Introduction

Since the advent of the famous first X-ray image of Mrs. Roentgen's hand in 1895, medicine has experienced an unprecedented revolution.[1] Physicians instantly recognized that the deep tissue penetration capability of X-rays, which could display internal anatomic structures of a patient without the need for surgical operations, would play an important role in medical diagnoses. X-ray examination is a noninvasive imaging procedure that does not damage tissues, is painless to the patient, and permits facile image processing.[2,3] Even with the recent phenomenal growth of other noninvasive imaging techniques including magnetic resonance imaging (MRI) and ultrasound (US), X-ray computed tomography (CT) remains the favored noninvasive

Published on the Web 09/05/2012 www.pubs.acs.org/accounts
10.1021/ar300150c

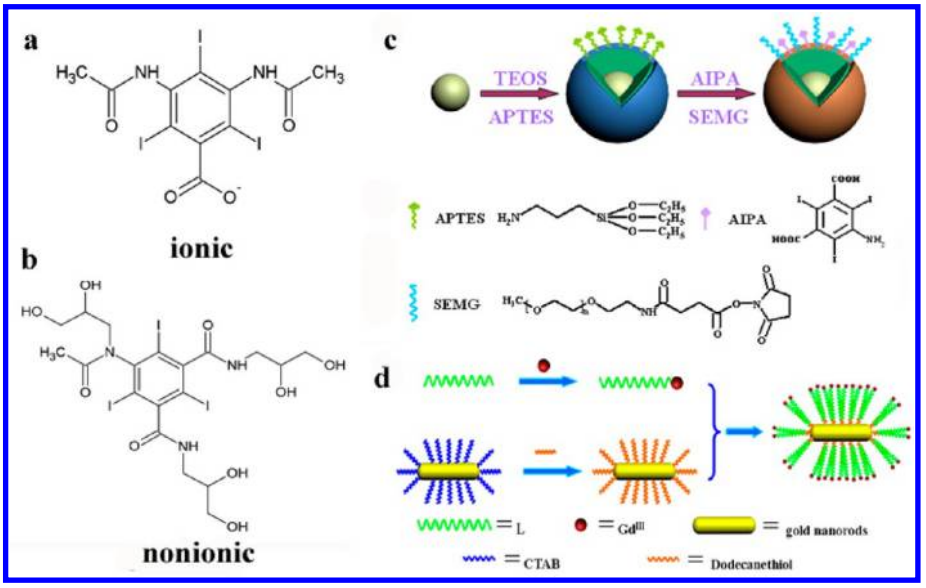

FIGURE 1. (a,b) Chemical structure of representative ionic and nonionic forms of clinical iodinated agents. (c,d) Schematic illustration of the synthesis of iodinated and Au NR-based nanoparticulate CT contrast agents, respectively. Figures reproduced with permission from refs 17, and 28. Copyright 2011 RSC Publishing.

approach in modern diagnostic medicine. According to IMV's 2011 CT Market Outlook Report, in 2010, an estimated 81.9 million CT procedures were performed in the United States.

Owing to the inherent contrast between electron-dense bones and the surrounding more permeable soft tissues, bone structures in the whole body can be superbly visualized under X-ray irradiation, but different soft tissues with similar densities cannot be distinguished by unenhanced X-ray imaging. Administration of contrast agents into patients better delineates these various tissues. Contrast agents exhibit differential uptake into different tissues where they effectively absorb the X-rays, affording transient contrast enhancement which can be visualized in the soft tissues with X-ray irradiation.[4] Currently, water-soluble aromatic iodinated molecules are routinely used for in vivo contrast enhancement in clinical settings.[5,6] Despite several generations of evolution, clinical iodinated agents are still hampered by three limitations: (i) due to the low molecular weight, they are rapidly excreted by the kidney, resulting in rather short circulation times in vivo; (ii) large doses of contrast agents are required for adequate visualization and their rapid renal elimination may lead to serious adverse effects; and (iii) although targeted biomolecules can be functionalized onto the iodinated molecules, targeted imaging with them is not possible due to the low payload that is being delivered in such instances and the low sensitivity of CT to contrast agents.

A long-sought-after CT contrast agent is the nanoparticle. In addition to the unique chemical and physical properties, nanoparticles have tunable composition, shape, and size, and they can be readily attached to bioconjugates with interesting biofunctionalities on their surface.[7,8] The nanosize itself makes nanoparticles particularly advantageous for biomedical applications.[9] When administered into living organisms, well-stabilized nanoparticles with size of 10−500 nm display very long blood circulation time. They can accumulate at the tumor sites via enhanced permeation and retention effect (EPR) or by active targeting of cancer cells, extending their applications to targeted imaging or therapy.[10,11] Conversely, small molecules or micrometer-sized particles can be removed quickly from the blood vessels by renal clearance and phagocytosis of reticuloendothelial system (RES), respectively.[12,13] Moreover, nanoparticles are ideal platforms for the design of multimodal imaging nanoprobes, since multiple diverse functions can be integrated into a single particle. Consequently, nanoparticulate imaging agents have attracted intense interest both in research and clinical applications.

The past two decades have witnessed a rapid increase in the design of nanoparticulate agents for MRI and fluorescence imaging (FI), and some particles have even been approved for clinical applications or are undergoing clinical verification. Nevertheless, the development of nanoparticles for X-ray CT imaging is still in the early stages, possibly attributing to the big challenge in the preparation of nanoparticulate CT contrast agents that must satisfy the following criteria simultaneously: (1) excellent biocompatibility; (2) high contrast efficacy; (3) cost effectiveness; (4) small size;

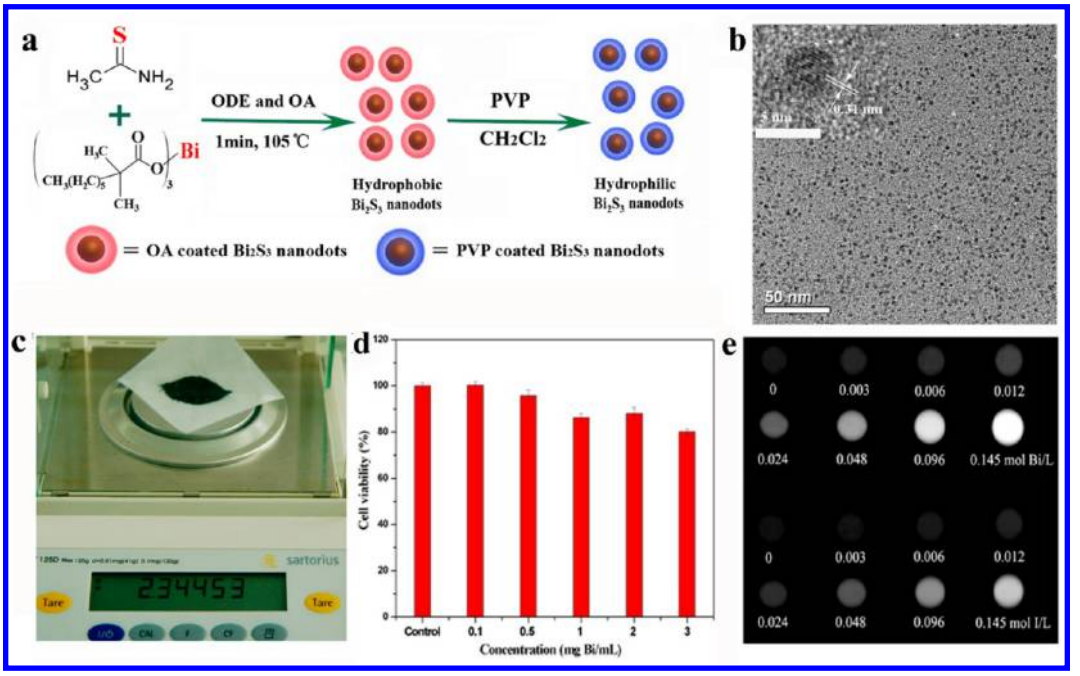

FIGURE 2. (a) Schematic illustration of the synthesis and surface modification of Bi_2S_3 nanodots. (b) TEM image of OA-Bi_2S_3 nanodots. (c) Large-scale production of Bi_2S_3 nanodots. (d) Cytotoxicity of PVP-Bi_2S_3 nanodots. (e) CT images of PVP-Bi_2S_3 nanodots and Iobitridol with different concentrations.[33]

(5) long in vivo circulation time; and (6) long-term colloidal stability in the physiological environment. This Account focuses mainly on our own efforts and strategies to develop novel nanoparticulate CT contrast agents that comply with the criteria mentioned above. We hope that this Account will help to accelerate further progress in this promising field.

2. Mechanism of X-ray CT Imaging

When an X-ray beam traverses a patient's body, the absorption of X-ray photons by the body reduces the X-ray beam intensity. This phenomenon is defined as X-ray attenuation and it is closely related with the mass attenuation coefficient (μ). Different tissues have distinctive μ values; thus, contrast occurs when an X-ray beam traverses different tissues and the larger the difference in μ values between tissues, the greater will be the contrast. Unfortunately, the difference in μ values among soft tissues in the human body is too small to delineate specific tissues under X-ray irradiation. Consequently, contrast agents that have differential uptake by different tissues are required.

Typically, X-ray attenuation results from three interactions occurring between X-ray photons and the traversed matter: coherent scattering, photoelectron effect, and Compton scattering. Coherent scattering is so small that it is commonly neglected. Compton scattering usually induces an increase in noise and a decrease in contrast. In practical applications, low-energy X-ray radiation results in exposing the patients to a high dose of radiation energy since most of the X-rays are absorbed. A proper increase in the X-ray energy can reduce the exposure dose. In this case, the contribution of Compton scattering to X-ray attenuation will diminish. Hence, the photoelectron effect will be the predominant contributor, and its contribution will be higher with absorbers of higher atomic number .[14,15] Also, the photoelectron effect causes a sharp increase in the mass attenuation coefficient at the K-shell electron binding energy (K-edge). Each element has its own characteristic K-edge value.

On the other hand, an X-ray spectrum generated at 150 KVp shows a maximum intensity around 45−50 KeV, and the characteristic radiation emitted is between 57 and 69 KeV.[14] Based on the above discussions, the X-ray attenuation of contrast agents will be enhanced by selecting the elements with higher atomic numbers and K-edge values within the X-ray spectrum.

3. Iodinated Nanoparticulate Contrast Agents

Currently, water-soluble iodinated molecules that utilize 1,3,5-triiodobenzene as a platform are widely used as clinical CT contrast agents, which are mainly distinguished as ionic and nonionic forms (Figure 1a,b). They can effectively absorb X-ray but suffer from the issues as demonstrated

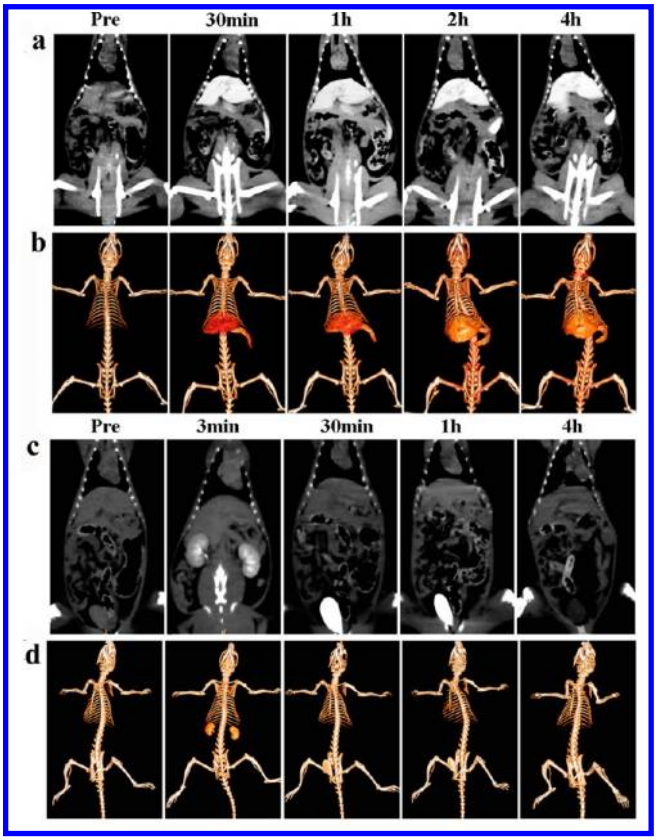

FIGURE 3. (a,c) Serial CT coronal views of a rat following intravenous injection of PVP-Bi_2S_3 solution and Iobitridol, respectively. (b,d) The corresponding 3D renderings of in vivo CT images above.[33]

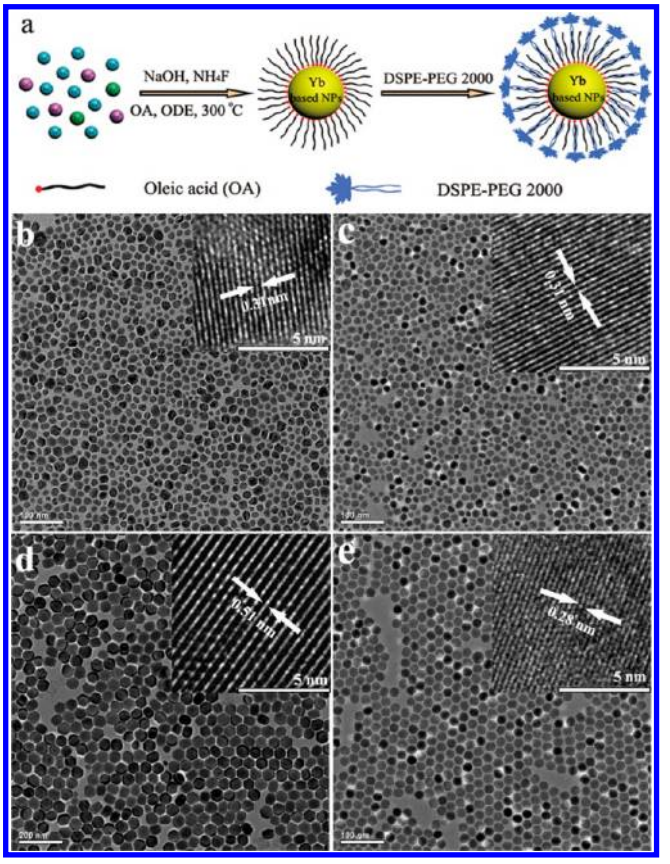

FIGURE 4. (a) Schematic illustration of the synthesis and surface modification of OA-UCNPs. (b–e) TEM and high-resolution TEM images of $NaYbF_4$:Er nanoparticles doped with (b) 0 mol %, (c) 10 mol %, (d) 20 mol %, and (e) 30 mol % of Gd.[39]

above, precluding their applications in angiography and targeted imaging. Conjugation of iodinated compounds with functionalized nanoparticles is an effective strategy to address these issues, since nanoparticles with sizes larger than 10 nm (normal renal filtration threshold) will be eliminated slowly from the body through a hepatobiliary/fecal route instead of via renal clearance.[16] Furthermore, selection of appropriate nanoparticles will enable the fabrication of multifunctional nanomedical platforms for multimodal imaging. With this in mind, lanthanide-doped upconversion luminescence nanoparticles (UCNPs) with an average diameter of 28 nm have been prepared and then encapsulated in a silica shell to impart water solubility and biocompatibility. 5-Amino-2,4,6-triiodoisophthalic acid was next attached to their surface, followed by linking poly(ethylene glycol) (PEG) to improve stability (Figure 1c).[17] Following intravenous injection of UCNPs@SiO_2–I/PEG into the rat, they showed prolonged circulation time in vivo, and liver contrast was observed even after 30 min. Besides, strong upconversion fluorescence of UCNPs@SiO_2–I/PEG can be used for biolabeling and guidance to surgical treatment.

Despite prolonged in vivo circulation time as compared to iodinated molecules, iodine-conjugated nanoparticles are still limited by iodine loading through surface covalent conjugation. The final concentration of iodine is relatively lower while the viscosity of the agent has been significantly increased. The preparation of iodinated nanoemulsions using iodine-functionalized amphiphilic polymer could effectively increase the iodine loading.[18–21] Nevertheless, when considering the X-ray spectrum and K-edge value of iodine (33 KeV), it can be concluded that iodine is not optimal for X-ray attenuation and thus determines the low contrast efficacy of these iodinated nanoemulsions. Moreover, iodinated agents cannot be used for those patients who are iodine hypersensitive. The development of a new generation of CT contrast agents using nanoparticles composed of other elements with higher X-ray attenuation remains a critical need. The design of new agents should also be guided by other criteria, for instance, low toxicity.

4. Metal-Based Nanoparticulate Contrast Agents

4.1. Gold-Based Nanoparticulate Contrast Agents. Gold has a higher atomic number than iodine, and thus, the

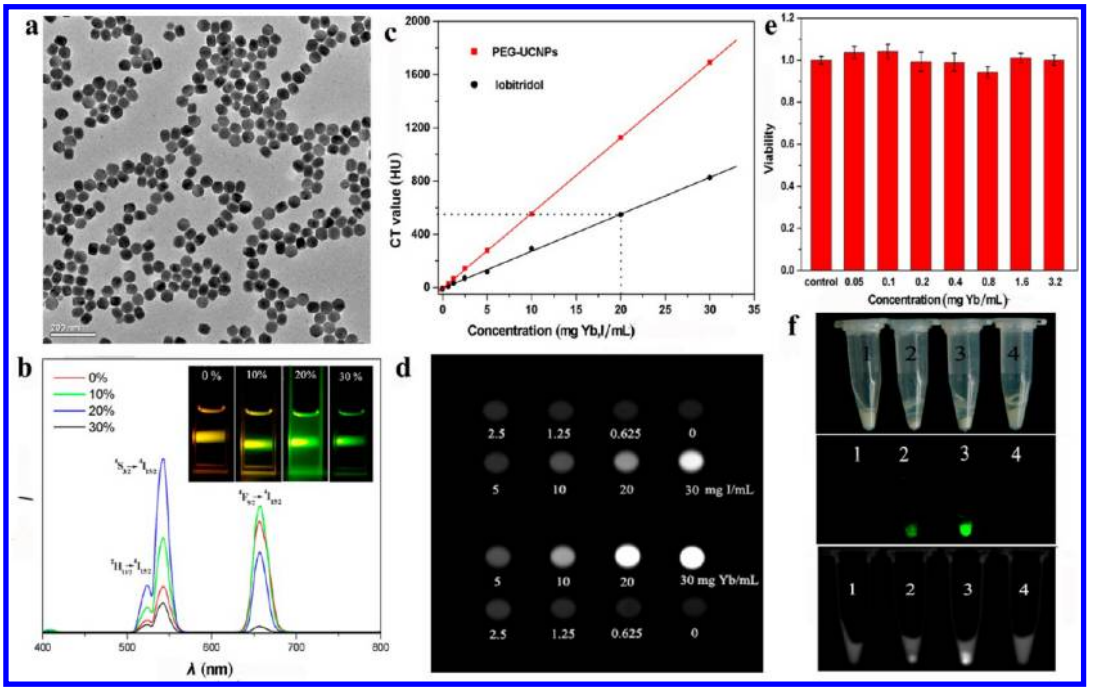

FIGURE 5. (a) TEM image of PEG-UCNPs. (b) Room-temperature upconversion luminescence spectra of Gd-doped UCNPs with different concentrations of Gd. (c) CT value of PEG-UCNPs and Iobitridol as a function of the concentration of Yb and I, respectively. (d) CT images of PEG-UCNPs solutions and Iobitridol with different concentrations of Yb and I. (e) Cytotoxicity of PEG-UCNPs. (f) Cellular imaging results of HeLa cells incubated with increased concentration of PEG-UCNPs and Iobitridol ((1) control, (2) 1.6, and (3) 3.2 mg Yb/mL; (4) 10 mg I/mL): bright image (top), upconversion luminescence image (middle), and CT image (bottom).[39]

contribution of photoelectron effect to X-ray attenuation with gold is larger. Moreover, Au nanostructures can package a larger number of the contrast element (Au) than iodine-based nanoparticles which are synthesized through surface covalent conjugation of iodinated molecules or polymerization of iodine functionalized amphiphilic molecules, thereby lowering the concentration of the agent. Besides, the size and shape of gold nanostructures can be easily controlled, and their surface can be modified with various functional groups. Gold is also chemically inert and is considered to be nontoxic in vivo.[22] Over the past few years, Au nanoparticles have attracted intense interest as CT contrast agents. They were readily functionalized with PEG or targeted proteins and have showed very long circulation time in vivo, low toxicity, and efficacy profiles comparable to or better than iodinated agents.[22−26] Compared to gold nanoparticles, gold nanorods (Au NRs) possess a lot of diverse and distinct properties, for instance, a strong surface plasmon resonance in the near-infrared (NIR) region.[27] Together with X-ray attenuation, Au NRs can be used for simultaneous diagnosis and therapy. Subsequent studies by our group explored Au NRs functionalized with Gd chelates for MR and CT bimodal imaging (Figure 1d).[28] They could induce significant enhancement both in CT and MR signals. Furthermore, their absorption in NIR allows them to act as promising photothermal therapy agents. Nevertheless, in contrast to MRI and photothermal therapy in which very low amounts of agents are used, CT imaging requires a much larger dose of Au NRs to achieve sufficient contrast effects. The price of gold becomes the huge obstacle to the commercialization of Au-based nanoparticulate CT contrast agents.

4.2. Bismuth-Based Nanoparticulate Contrast Agents. Relative to Au, bismuth (Bi) is less expensive. Bi possesses larger X-ray attenuation coefficient, has low toxicity, and leaves no residue in the organism. In 2009, Lanza's group reported a soft Bi-encapsulated polymeric nanoparticle with a high metal content, which offered several-fold CT signal enhancement in suspension and in vivo demonstrating detection sensitivity reaching to the low nanomolar particulate concentration range.[29] Another promising Bi-based contrast agent is the relatively hard Bi-containing nanoparticle, Bi_2S_3. The earliest report involving the use of Bi_2S_3 nanoparticles as a CT contrast agent appeared in 2006.[30] However, the exploration of Bi_2S_3-based CT contrast agents has been hampered at its early stage due to the challenges in their controlled synthesis and surface modification.

Hydrothermal methods were commonly employed to synthesize Bi_2S_3 nanostructures previously;[31] this procedure

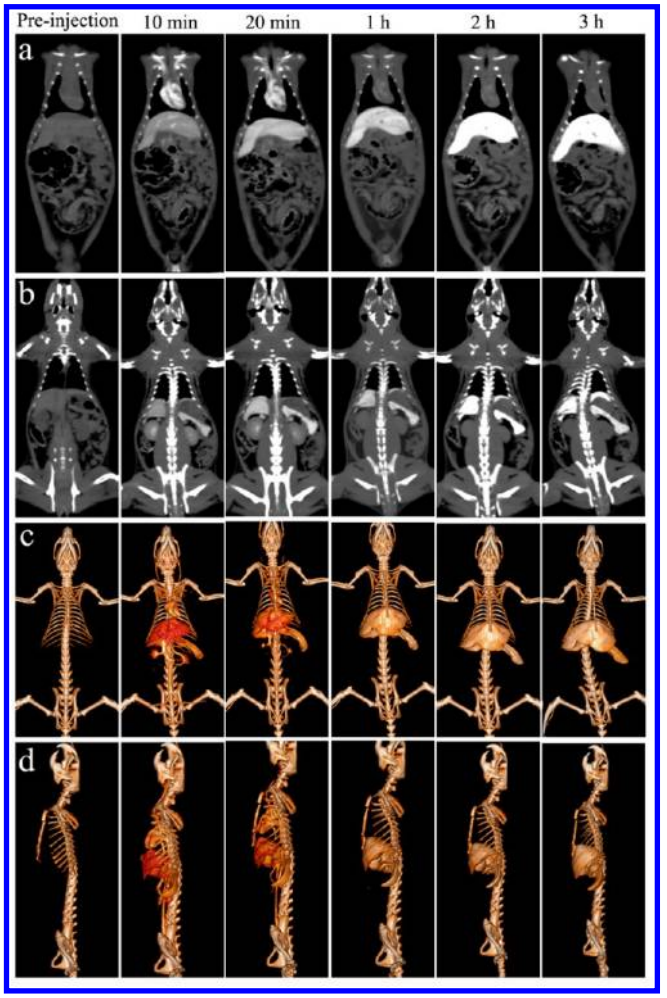

FIGURE 6. (a,b) CT coronal view images of a rat after intravenous injection of PEG-UCNPs solution at timed intervals. (c,d) Corresponding 3D renderings of in vivo CT images.[39]

has generally yielded nanoparticles with wide size distribution and poor monodispersity. Alternatively, an emerging "hot injection" method with oleyl amine (OAm) as both ligand and solvent can produce uniformly sized Bi_2S_3 nanoparticles.[32] The use of OAm in this strategy led to two major problems: (1) reduction of Bi^{3+} ions to metallic Bi with high chemical activity, and (2) aggregation of nanoparticles resulting from the detachment of OAm from the surface of Bi_2S_3 during following washing processes, which was attributed to the weak coordination interaction between OAm and Bi_2S_3. These problems were overcome by utilizing oleic acid (OA) as the coordination ligand instead of OAm. The carboxylic group of OA can strongly bind to Bi^{3+} ions, effectively preventing Bi_2S_3 nanoparticles from aggregating and avoiding the reduction of Bi ions. Pure Bi_2S_3 nanodots with remarkable size uniformity (2−3 nm) and monodispersity were produced (Figure 2a,b).[33] These small Bi_2S_3 nanodots are more suitable than large particles for biological and medical applications, particularly for labeling subcellular organelle or proteins, because they are less likely to disturb their biological functions and unlikely to be rapidly recognized and cleared by phagocytes.[34] Of particular importance is the versatility of this approach: preparation of pure Bi_2S_3 nanodots can be easily scaled up by increasing the amount of reactants (Figure 2c).

As the controlled synthesis of Bi_2S_3 is now well established, difficulties with its surface modification still remained. We subsequently described a facile ligand exchange method for modification of hydrophobic Bi_2S_3 nanodots with biocompatible poly(vinylpyrrolidone) (PVP). After ligand exchange, PVP-Bi_2S_3 nanodots showed excellent colloidal stability, low cytotoxicity and provided a contrast efficacy 1.9 time higher than that of Iobitridol (a widely used clinical agent) (Figure 2d,e).

The feasibility of PVP-Bi_2S_3 nanodots as an in vivo CT contrast agent was tested by intravenous injection of PVP-Bi_2S_3 solution into a rat followed by imaging with a clinical CT scanner at indicated time intervals (Figure 3). Clear contrast enhancement of several organs including heart, liver, and spleen could be observed. The signal contrast enhancement of the heart persisted for 1 h, while liver and spleen were clearly delineated from the surrounding tissues even after 4 h. Conversely, following intravenous injection of Iobitridol into a different rat, no enhancement in these organs was detected, even at 3 min postinjection. Most of Iobitridol had accumulated in the kidney and bladder. These results demonstrated the longer in vivo circulation time of PVP-Bi_2S_3 nanodots synthesized by our strategy and indicated their potential applications in vascular imaging and detection of hepatic metastases. Thereafter, Sailor and co-workers reported a similar method to produced Bi_2S_3 nanoparticles. By coating them with targeted peptide, Bi_2S_3 nanoparticles were successfully used for breast cancer targeted imaging.[35]

4.3. Ytterbium-Based Nanoparticulate Contrast Agents. Apart from Au and Bi, Pt- and Ta-based nanoparticles have also been investigated as CT contrast agents.[36−38] They have shown strong contrast. For instance, the contrast efficacy of Ta is about 1.4 times higher than that of iodine. Despite good imaging effects, acceptable safety profiles and long circulation times in vivo, we believe there is still room for improvement in the case of contrast efficacy of contrast agents. Au, Bi, Pt, and Ta all have higher atomic numbers relative to iodine, and, in principle, they should all produce larger photoelectron effects. However, this does not necessarily mean that they will give significantly enhanced X-ray

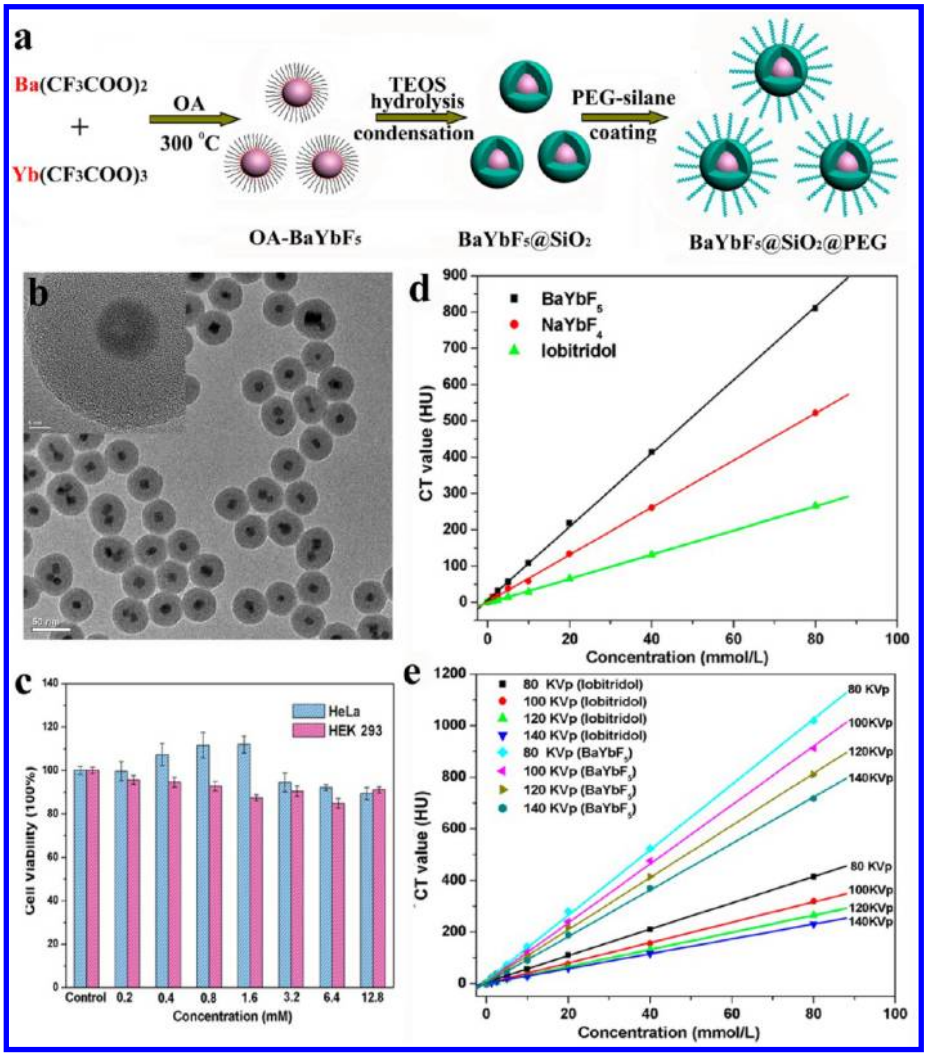

FIGURE 7. (a) Schematic illustration of the synthesis of $BaYbF_5$@SiO_2@PEG. (b) TEM and high-resolution TEM images of $BaYbF_5$@SiO_2@PEG. (c) Cell viability of HEK 293 and HeLa cells after incubation with increased concentration of $BaYbF_5$@SiO_2@PEG for 24 h. (d) CT values of $BaYbF_5$@SiO_2@PEG, $NaYbF_4$@PEG and Iobitridol with different concentrations of Yb/iodine at 120 KVp. (e) CT values of $BaYbF_5$@SiO_2@PEG and Iobitridol with different concentrations at different voltages.[42]

attenuation in clinical settings. As discussed above, photoelectric effect also explains the sharp increase in mass attenuation coefficients at the K-edge. Comparing the K-edges of these metal elements (81, 78, 91, and 67 KeV for Au, Pt, Bi, and Ta, respectively) with the X-ray spectrum, we observe that the K-edge values of these metal elements, similar to the case of iodine (33 KeV), deviate from the higher-intensity region of X-ray spectrum, thus contributing limited X-ray attenuation. If the K-edge value of a specific element is located just within this region, more X-ray will be absorbed. In other words, this element shows larger X-ray attenuation. Thus, the first example of Yb-based nanoparticulate CT contrast agents was described recently (Figure 4a).[39] The greatest benefit of Yb is its proper K-edge energy (61 keV) that is located just within the higher-intensity region of the X-ray spectrum at 120 KVp, a commonly used voltage in clinical CT, hence ensuring higher intrinsic contrast. Other factors such as low toxicity when encapsulated in the stable nanoparticle and higher abundance in the earth's crust than the other above metals allow Yb-based nanoparticles to satisfy the criteria for efficient nanoparticulate CT contrast agents.

The size, shape, and surface properties of nanoparticles govern their interactions with cells, and thus, it is desirable to keep nanoparticles uniform both in size and shape. By doping different amounts of Gd^{3+} ions during the synthetic process, the size and shape of oleic acid stabilized $NaYbF_4$:Er nanoparticles (OA-UCNPs) can be easily controlled (Figure 4b–e). Subsequently, OA-UCNPs were modified with DSPE-PEG2000 through hydrophobic interaction between DSPE-PEG2000

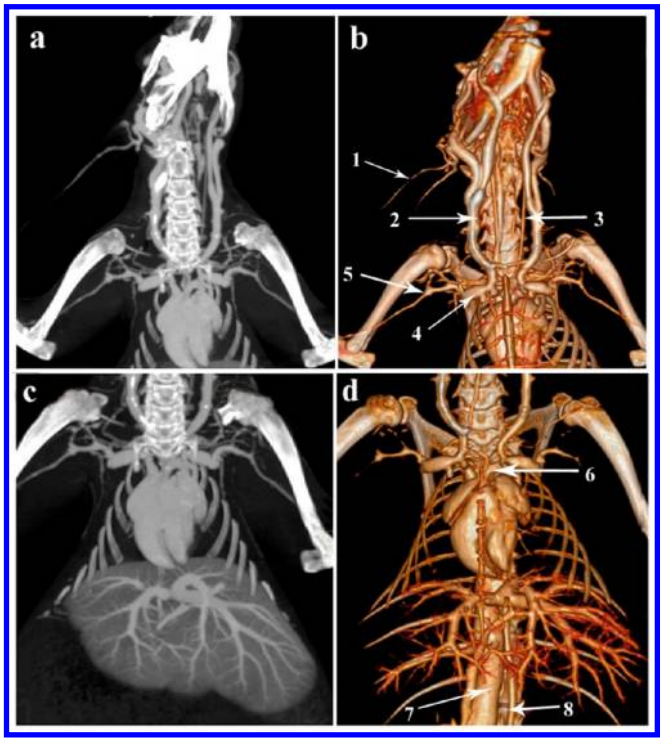

FIGURE 8. High-resolution blood pool CT images of the rabbit collected at 10 min after intravenous injection of $BaYbF_5$@SiO_2@PEG solution. (a,c) Coronal view images and (b,d) corresponding 3D renderings of CT images. The arrows indicate several great vessels: (1) auricular vein, (2) jugular vein, (3) carotid artery, (4) subclavian vein, (5) axillary vein, (6) aortic arch, (7) inferior vena cava, and (8) aorta.[42]

and OA to impart water solubility. PEG coating can also improve circulation time in blood and help to reduce the nonspecific binding.[40] The obtained PEG-UCNPs remained monodisperse in water (Figure 5a). Notably, PEG-UCNPs have negligible cytotoxicity even at an extremely high concentrations (Figure 5e), and no leaching of free Yb^{3+} or Gd^{3+} ions occurs even after 1 week dialysis in blood serum and physiological saline. Furthermore, they can be internalized by HeLa cells, and the internalization was dose-dependent (Figure 5f). This internalization is of great importance in clinical applications, particularly for tumor targeted imaging and detection. Conversely, hardly any uptake by cells was observed for Iobitridol even at a concentration three times higher than that of Yb due to its small molecular weight.

The contrast efficacy of PEG-UCNPs was then investigated. At equivalent concentrations, PEG-UCNPs provided higher X-ray absorption compared to Iobitridol (Figure 5c,d), even superior to currently available Au-, Pt-, Bi-, and Ta-based nanoparticulate CT contrast agents at 120 KVp owing to the K-edge value of Yb that matches the X-ray spectrum. After intravenous administration of PEG-UCNPs into a rat, a clearer enhancement of the signal of the heart could be observed at least within 20 min without an appreciable loss of contrast relative to PVP-Bi_2S_3 nanodots. Close inspection of the 3D-renderings of CT images showed evident contrast in the great vessels within this same period of time as well. Likewise, long-lasting liver and spleen-signal enhancement could be still visualized (Figure 6). Additionally, similar findings were observed when the dosage of PEG-UCNPs was reduced by a half. This reduced dose requirement is highly beneficial in a contrast agent, because it can effectively decrease potential adverse effects in patients.

The benefit of PEG-UCNPs is not limited to X-ray attenuation; rather, these nanoparticles are also well-known for their upconversion luminescence (UCL). UCL displays a great penetration depth in biological tissues, low phototoxicity, and reduced background.[41] Interestingly, Gd doping could induce a significant enhancement of the green UCL intensity (Figure 5b). Moreover, the emission could be tuned to the NIR region, further avoiding the poor tissue penetration and the scattering of large amounts of visible wavelengths. Gd doping can not only enhance the UCL intensity, but also endow PEG-UCNPs with MRI capability. Such multimodal imaging capability is highly useful for both noninvasive diagnosis and guidance in surgical treatment.

4.4. Binary Contrast Agents. Great efforts by us and others have been devoted to the improvement of contrast efficacy and in vivo imaging performance of CT contrast agents. Nevertheless, there are still limitations associated with these contrast agents because they cannot always display great superiority to clinical iodinated agents. In clinical CT examination, the operating voltage changes from 80 to 140 KVp depending on the applications. For instance, when the patients are children, the operating voltage must be adjusted to 80 KVp, whereas for the overweighted patients, it will be set at 140 KVp in order to acquire valuable diagnosis information. In these cases, the contrast efficacy of PEG-UCNPs, including other metals-based agents, is still not optimal. At a specific voltage, these metal elements, together with iodine, will display greatly differential X-ray attenuation due to their large differences in K-edge values. As operating voltage changes, X-ray attenuation of each element will also change. The change of operating voltage will also induce a shift of the higher-intensity region in X-ray spectrum. Generally, at 80 KVp, the contrast efficacy of currently available nanoparticulate contrast agents is lower compared to iodinated molecules, because the small K-edge value of iodine will be closer to the higher-intensity region of X-ray spectrum. Nevertheless, iodinated agents suffers from limitations as mentioned above. Thus, engineering

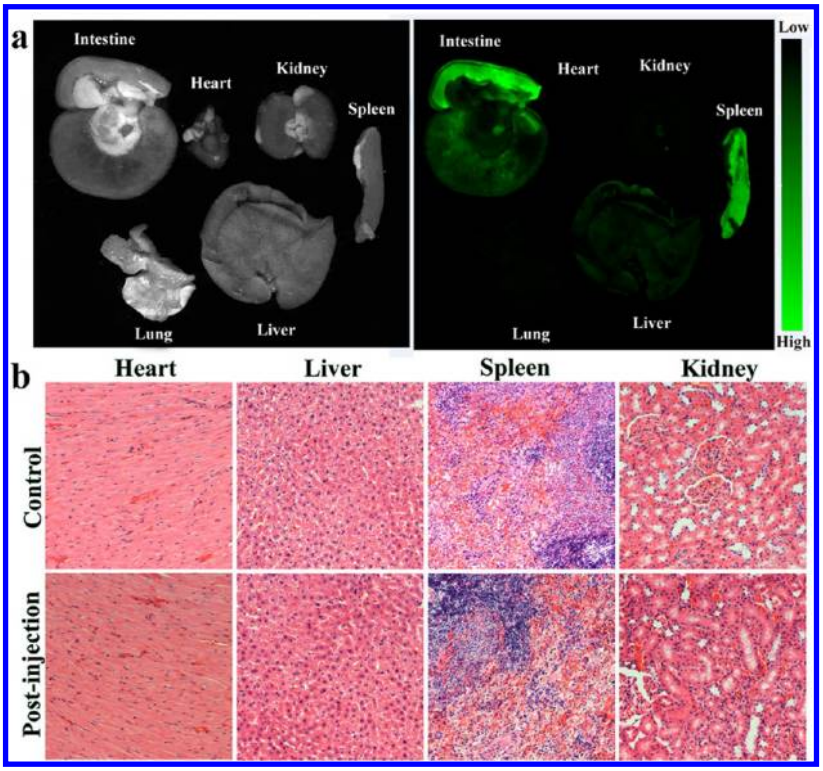

FIGURE 9. (a) Biodistribution of $BaYbF_5$(FITC)@SiO_2@PEG in the rat 24 postinjection of $BaYbF_5$(FITC)@SiO_2@PEG. Left: white light photograph. Right: fluorescence image of several organs. (b) Histological section of the heart, liver, spleen, and kidney of the rat 1 month after intravenous injection of a single dose of $BaYbF_5$@SiO_2@PEG solution. Sections are stained with H&E and observed under a light microscope at 100× magnification.[42]

novel nanoparticulate contrast agents that have longer in vivo circulation time and higher contrast efficacy at different operating voltages relative to clinical iodinated agents is desired.

The currently available nanoparticulate CT contrast agents contain a single element that contributes to X-ray attenuation, for instance, Au, Bi, and Ta in Au, Bi_2S_3, and TaOx nanoparticles. The presence of a single contrast element can only provide limited contrast efficacy and cannot be tailored to the changes of operating voltage. This concern could be addressed via engineering nanoparticles composed of multiple elements with differential K-edge values within X-ray spectrum. With this in mind, $BaYbF_5$ nanoparticles containing two contrast elements with differential K-edge values (61 and 37 KeV for Yb and Ba, respectively) were recently reported as the first example of binary contrast agents.[42] For biomedical applications, $BaYbF_5$ nanoparticles were coated with a silica shell to impart water solubility, and then passivated with PEG-silane to reduce nonspecific adsorption of proteins and interactions of surface silanols with cellular membranes (Figure 7a). After silica coating, the overall size of $BaYbF_5$@SiO_2@PEG is still less than 100 nm, and they can also be well dispersed in water with long-term colloidal stability and no leaching of free Ba^{2+} and Yb^{3+} ions (Figure 7b). Due to the excellent biocompatibility of silica, $BaYbF_5$@SiO_2@PEG exhibited remarkably low cytotoxicity. Neither the cell viability nor the proliferation was hindered by the presence of $BaYbF_5$@SiO_2@PEG for both HeLa and HEK 293 cells even at the highest tested concentration (Figure 7c).

As expected, the presence of two contrast elements in $BaYbF_5$@SiO_2@PEG enabled remarkable enhancement in X-ray attenuation compared to Iobitridol and $NaYbF_4$@PEG that has a single contrast element (Figure 7d). Despite about 30% decrease in the contrast when the voltage increased from 80 to 140 KVp, $BaYbF_5$@SiO_2@PEG maintained higher X-ray attenuation than Iobitridol (Figure 7e). This improvement in contrast efficacy confirmed the speculation above and revealed the superiority of $BaYbF_5$@SiO_2@PEG as a new generation of CT contrast agent.

The high colloidal stability arising from PEG coating enabled a long retention time of $BaYbF_5$@SiO_2@PEG in the vasculature. In our preliminary observations, after treatment of $BaYbF_5$@SiO_2@PEG, the signal in the vasculature of the rat was immediately enhanced and visualization of the bright signal persisted for at least 2 h. Such a long-lasting

signal in blood was not realized in our previous studies and is quite long enough for blood pool CT imaging (angiography). Angiography is very important in clinical applications because it can detect many diseases including myocardial infarction, atherosclerotic plaques, and thrombosis.[43] High-resolution blood pool CT images were obtained after intravenous injection of $BaYbF_5$@SiO_2@PEG solution into a large animal model, the rabbit (Figure 8). At 10 min postinjection, various blood vessels were clearly visualized in CT images. Even after 1 h, the bright signal of these blood vessels remained. By tracking the nanoparticles in the rat body following treatment of FITC-labeled $BaYbF_5$@SiO_2@PEG, most nanoparticles were found to have been eliminated from the blood pool and accumulated in the liver and spleen through the reticuloendothelial system at 24 h postinjection (Figure 9a), and one month later most of them have been eliminated from the rat body through a hepatobiliary/fecal route. During this time, no harmful effect or organ damage associated with administration of $BaYbF_5$@SiO_2@PEG could be detected (Figure 9b).

5. Conclusions and Perspectives

Over the past decade, nanoparticles have been developed for biological and biomedical applications. Although the initial research on nanoparticulate CT contrast agents first appeared in the late 1990s, advances in this area have lagged far behind other imaging methodologies such as MRI and FI. In this Account, we described our rational strategies in the design of several nanoparticles as novel CT contrast agents for in vivo X-ray CT imaging. The studies featured herein attempt to, in particular, shed light on the improvements of contrast efficacy and imaging performance in vivo of nanoparticulate agents. By optimizing the contrast element in nanoparticles based on the mechanism of X-ray CT imaging, we synthesized a novel Yb-based nanoparticulate CT contrast agent that has the contrast efficacy higher than clinical iodinated agents, even superior to currently available Au-, Pt-, Bi-, and Ta-based nanoparticulate CT contrast agents at 120 kVp. Furthermore, through integrating both Ba and Yb with differential K-edge values into a single nanoparticle, we developed the first example of binary contrast agents that provided a much higher contrast efficacy compared to Iobitridol at different voltages, making this binary contrast agent highly suited to diagnostic imaging of various patients. Due to the significantly prolonged circulation time in vivo, its applications could be extended to angiography to detect many serious diseases.

Despite exciting progress, it is fair to admit that the development of nanoparticulate CT contrast agents is still at a relatively early stage. The studies in this Account just focused on imaging. Current trends are directed toward the development of multifunctional nanomedical platforms for targeted imaging or simultaneous diagnosis and therapy. Multifunctional nanoparticulate agents must be modified with both targeting ligands and therapeutic agents. Issues such as in vivo targeting and therapy efficiency, long-term stability as well as in-depth investigations of the toxicology and excretion of the functionalized nanoparticles should be clearly addressed. Once these issues are successfully resolved, these nanoparticulate agents will provide physicians with important new tools for diagnosis and efficient treatment of diseases.

We would like to thank our co-workers past and present who contributed to the results described in this Account. This work is supported by NSFC (Nos. 21125521, 21075117), the National Basic Research Program of China (973 Program, No. 2010CB933600), and the "Hundred Talents Project" of CAS.

Supporting Information. Detailed experimental methods. This material is available free of charge via the Internet at http://pubs.acs.org.

BIOGRAPHICAL INFORMATION

Yanlan Liu received her B.S. in chemistry from Heilongjiang University, China, in 2008. She is pursuing her Ph.D. under the direction of Professor Lu. Her current research interests focus on the development of novel multifunctional nanomaterials for bioimaging and therapy.

Kelong Ai received his B.S. in Environmental Sciences from Wuhan University, China, in 2002, and then joined professor Lu's group as an Assistant professor. He has a broad range of research interests in biosensing and bioimaging.

Lehui Lu received his M.S. (2000) and Ph.D. (2003) from the Changchun Institute of Applied Chemistry, Chinese Academy of Sciences (CIACCAS). He carried out his postdoctoral research at Hamburg University (2003−2005) and Kwansei Gakuin University (2005−2007). He is currently a professor at CIACCAS, where he is also the Director of the State Key Laboratory of Electroanalytical Chemistry.

FOOTNOTES

*To whom correspondence should be addressed. E-mail: lehuilu@ciac.jl.cn.
The authors declare no competing financial interest.

REFERENCES

1 Roentgen, W. C. On a New Kind of Rays. *Sitzungsber. Phys.-Med. Ges. Wurzburg* **1895**, *137*, S132–1141.

2 Schwenzer, N. F.; Springer, F.; Schraml, C.; Stefan, N.; Machann, J.; Schick, F. Non-invasive Assessment and Quantification of Liver Steatosis by Ultrasound, Computed Tomography and Magnetic Resonance. *J. Hepatol.* **2009**, *51*, 433–445.

3 deKrafft, K. E.; Xie, Z.; Cao, G.; Tran, S.; Ma, L.; Zhou, O. Z.; Lin, W. Iodinated Nanoscale Coordination Polymers as Potential Contrast Agents for Computed Tomography. *Angew. Chem., Int. Ed.* **2009**, *48*, 9901–9904.

4 Kalender, W. A. X-ray Computed Tomography. *Phys. Med. Biol.* **2006**, *51*, R29–R43.

5 Christiansen, C. X-ray Contrast Media-An Overview. *Toxicology* **2005**, *209*, 185–187.

6 Krause, W.; Schneider, P. W. Chemistry of X-ray Contrast Agents. *Top. Curr. Chem.* **2002**, *222*, 107–150.

7 Brannon-Peppas, L.; Blanchette, J. O. Nanoparticle and Targeted Systems for Cancer Therapy. *Adv. Drug Delivery Rev.* **2004**, *56*, 1649–1659.

8 Park, K.; Lee, S.; Kang, E.; Kim, K.; Choi, K.; Kwon, I. C. New Generation of Multifunctional Nanoparticles for Cancer Imaging and Therapy. *Adv. Funct. Mater.* **2009**, *19*, 1553–1566.

9 Lee, J. E.; Lee, N.; Kim, T.; Kim, J.; Hyeon, T. Multifunctional Mesoporous Silica Nanocomposite Nanoparticles for Theranostic Applications. *Acc. Chem. Res.* **2011**, *44*, 893–902.

10 Koo, H.; Huh, M. S.; Sun, I.-C.; Yuk, S. H.; Choi, K.; Kim, K.; Kwon, I. C. In Vivo Targeted Delivery of Nanoparticles for Theranosis. *Acc. Chem. Res.* **2011**, *44*, 1018–1028.

11 Peer, D.; Karp, J. M.; Hong, S.; Farokhzad, O. C.; Margalit, R.; Langer, R. Nanocarriers as an Emerging Platform for Cancer Therapy. *Nat. Nanotechnol.* **2007**, *2*, 751–760.

12 Chou, L. Y. T.; Ming, K.; Chan, W. C. W. Strategies for the Intracellular Delivery of Nanoparticles. *Chem. Soc. Rev.* **2011**, *40*, 233–245.

13 Popovic, Z.; Liu, W.; Chauhan, V. P.; Lee, J.; Wong, C.; Greytak, A. B.; Insin, N.; Nocera, D. G.; Fukumura, D.; Jain, R. K.; Bawendi, M. G. A Nanoparticle Size Series for In Vivo Fluorescence Imaging. *Angew. Chem., Int. Ed.* **2010**, *49*, 8649–8652.

14 Yu, S.-B.; Watson, A. D. Metal-based X-ray Contrast Media. *Chem. Rev.* **1999**, *99*, 2353–2377.

15 Pan, D.; Roessl, E.; Schlomka, J.-P.; Caruthers, S. D.; Senpan, A.; Scott, M. J.; Allen, J. S.; Zhang, H.; Hu, G.; Gaffney, P. J.; Choi, E. T.; Rasche, V.; Wickline, S. A.; Proksa, R.; Lanza, G. M. Computed Tomography in Color: NanoK-Enhanced Spectral CT Molecular Imaging. *Angew. Chem., Int. Ed.* **2010**, *49*, 9635–9639.

16 Longmire, M.; Choyke, P. L.; Kobayashi, H. Clearance Properties of Nano-sized Particles and Molecules as Imaging Agents: Considerations and Caveats. *Nanomedicine (London, U.K.)* **2008**, *3*, 703–717.

17 Zhang, G.; Liu, Y. L.; Yuan, Q. H.; Zong, C. H.; Liu, J. H.; Lu, L. H. Dual Modal In Vivo Imaging Using Upconversion Luminescence and Enhanced Computed Tomography Properties. *Nanoscale* **2011**, *3*, 4365–4371.

18 Konga, W. H.; Lee, W. J.; Cui, Z. Y.; Bae, K. H.; Park, T. G.; Kim, J. H.; Park, K.; Seo, S. W. Nanoparticulate Carrier Containing Water-Insoluble Iodinated Oil as a Multifunctional Contrast Agent for Computed Tomography Imaging. *Biomaterials* **2007**, *28*, 5555–5561.

19 Hallouard, F.; Anton, N.; Choquet, P.; Constantinesco, A.; Vandamme, T. Iodinated Blood Pool Contrast Media for Preclinical X-ray Imaging Applications-A Review. *Biomaterials* **2010**, *31*, 6249–6268.

20 de Vries, A.; Lub, E.; Custers, J.; van den Bosch, S.; Nicolay, K.; Grüll, H. Block-Copolymer-Stabilized Iodinated Emulsions for Use as CT Contrast Agents. *Biomaterials* **2010**, *31*, 6537–6544.

21 Hyafil, F.; Cornily, J.-C.; Feig, J. E.; Gordon, R.; Vucic, E.; Amirbekian, V.; Fisher, E. A.; Fuster, V.; Feldman, L. J.; Fayad, Z. A. Noninvasive Detection of Macrophages Using a Nanoparticulate Contrast Agent for Computed Tomography. *Nat. Med.* **2007**, *13*, 636–641.

22 Kim, D.; Park, S.; Lee, J. H.; Jeong, Y. Y.; Jon, S. Antibiofouling Polymer-Coated Gold Nanoparticles as a Contrast Agent for In Vivo X-ray Computed Tomography Imaging. *J. Am. Chem. Soc.* **2007**, *129*, 7661–7665.

23 Eck, W.; Nicholson, A. I.; Zentgraf, H.; Semmler, W.; Bartling, S. Anti-CD4-Targeted Gold Nanoparticles Induce Specific Contrast Enhancement of Peripheral Lymph Nodes in X-ray Computed Tomography of Live Mice. *Nano Lett.* **2010**, *10*, 2318–2322.

24 Sun, I.-C.; Eun, D.-K.; Koo, H.; Ko, C.-Y.; Kim, H.-S.; Yi, D. K.; Choi, K.; Kwon, I. C.; Kim, K.; Ahn, C.-H. Tumor-Targeting Gold Particles for Dual Computed Tomography/Optical Cancer Imaging. *Angew. Chem., Int. Ed.* **2011**, *50*, 9348–9351.

25 Kim, D.; Jeong, Y. Y.; Jon, S. A Drug-Loaded Aptamer-Gold Nanoparticle Bioconjugate for Combined CT Imaging and Therapy of Prostate Cancer. *ACS Nano* **2010**, *4*, 3689–3696.

26 Xu, C. J.; Tung, G. A.; Sun, S. H. Size and Concentration Effect of Gold Nanoparticles on X-ray Attenuation as Measured on Computed Tomography. *Chem. Mater.* **2008**, *20*, 4167–4169.

27 Huang, X.; El-Sayed, I. H.; Qian, W.; El-Sayed, M. A. Cancer Cell Imaging and Photothermal Therapy in the Near-Infrared Region by Using Gold Nanorods. *J. Am. Chem. Soc.* **2006**, *128*, 2115–2120.

28 Sun, H. M.; Yuan, Q. H.; Zhang, B. H.; Ai, K. L.; Zhang, P. G.; Lu, L. H. Gd^{III} Functionalized Gold Nanorods for Multimodal Imaging Applications. *Nanoscale* **2011**, *3*, 1990–1996.

29 Pan, D.; Williams, T. A.; Senpan, A.; Allen, J. S.; Scott, M. J.; Gaffney, P. J.; Wickline, S. A.; Lanza, G. M. Detecting Vascular Biosignatures with a Colloidal, Radio-Opaque Polymeric Nanoparticle. *J. Am. Chem. Soc.* **2009**, *131*, 15522–15527.

30 Rabin, O.; Perez, J. M.; Grimm, J.; Wojtkiewicz, G.; Weissleder, R. An X-ray Computed Tomography Imaging Agent Based on Long-Circulating Bismuth Sulphide Nanoparticles. *Nat. Mater.* **2006**, *5*, 118–122.

31 Sigman, M. B., Jr.; Korgel, B. A. Solventless Synthesis of Bi_2S_3 (Bismuthinite) Nanorods, Nanowires, and Nanofabric. *Chem. Mater.* **2005**, *17*, 1655–1660.

32 Malakooti, R.; Cademartiri, L.; Akçakir, Y.; Petrov, S.; Migliori, A.; Ozin, G. A. Shape-Controlled Bi_2S_3 Nanocrystals and Their Plasma Polymerization into Flexible Films. *Adv. Mater.* **2006**, *18*, 2189–2194.

33 Ai, K. L.; Liu, Y. L.; Liu, J. H.; Yuan, Q. H.; He, Y. Y.; Lu, L. H. Large-Scale Synthesis of Bi_2S_3 Nanodots as a Contrast Agent for In Vivo X-ray Computed Tomography Imaging. *Adv. Mater.* **2011**, *23*, 4886–4891.

34 Liu, Y. L.; Ai, K. L.; Yuan, Q. H.; Lu, L. H. Fluorescence-Enhanced Gadolinium-Doped Zinc Oxide Quantum Dots for Magnetic Resonance and Fluorescence Imaging. *Biomaterials* **2011**, *32*, 1185–1192.

35 Kinsella, J. M.; Jimenez, R. E.; Karmali, P. P.; Rush, A. M.; Kotamraju, V. R.; Gianneschi, N. C.; Ruoslahti, E.; Stupack, D. Sailor, M. J. X-Ray Computed Tomography Imaging of Breast Cancer by Using Targeted Peptide-Labeled Bismuth Sulfide Nanoparticles. *Angew. Chem., Int. Ed.* **2011**, *50*, 12308–12311.

36 Chou, S.-W.; Shau, Y.-H.; Wu, P.-C.; Yang, Y.-S.; Shieh, D.-B.; Chen, C.-C. In Vitro and In Vivo Studies of FePt Nanoparticles for Dual Modal CT/MRI Molecular Imaging. *J. Am. Chem. Soc.* **2010**, *132*, 13270–13278.

37 Oh, M. H.; Lee, N.; Kim, H.; Park, S. P.; Piao, Y.; Lee, J.; Jun, S. W.; Moon, W. K.; Choi, S. H.; Hyeon, T. Large-Scale Synthesis of Bioinert Tantalum Oxide Nanoparticles for X-ray Computed Tomography Imaging and Bimodal Image-Guided Sentinel Lymph Node Mapping. *J. Am. Chem. Soc.* **2011**, *133*, 5508–5515.

38 Bonitatibus, P. J., Jr.; Torres, A. S.; Goddard, G. D.; FitzGerald, P. F.; Kulkarni, A. M. Synthesis, Characterization, and Computed Tomography Imaging of a Tantalum Oxide Nanoparticle Imaging Agent. *Chem. Commun.* **2010**, *46*, 8956–8958.

39 Liu, Y. L.; Ai, K. L.; Liu, J. H.; Yuan, Q. H.; He, Y. Y.; Lu, L. H. A High-Performance Ytterbium-Based Nanoparticulate Contrast Agent for In Vivo X-ray Computed Tomography Imaging. *Angew. Chem., Int. Ed.* **2012**, *51*, 1437–1442.

40 Bardhan, R.; Lal, S.; Joshi, A.; Halas, N. J. Theranostic Nanoshells: from Probe Design to Imaging and Treatment of Cancer. *Acc. Chem. Res.* **2011**, *44*, 893–902.

41 Li, Z. Q.; Zhang, Y.; Jiang, S. Multicolor Core/Shell-Structured Upconversion Fluorescent Nanoparticles. *Adv. Mater.* **2008**, *20*, 4765–4769.

42 Liu, Y. L.; Ai, K. L.; Liu, J. H.; Yuan, Q. H.; He, Y. Y.; Lu, L. H. Hybrid $BaYbF_5$ Nanoparticles: Novel Binary Contrast agent for High-Resolution In Vivo X-ray Computed Tomography Angiography. *Adv. Healthcare Mater.* **2012**, *1*, 461–466.

43 Kim, B. H.; Lee, N.; Kim, H.; An, K.; Park, Y.; Choi, Y.; Shin, K.; Lee, Y.; Kwon, S. G.; Na, H. B.; Park, J.; Ahn, T. Y.; Kim, Y. W.; Moon, W. K.; Choi, S. H.; Hyeon, T. Large-Scale Synthesis of Uniform and Extremely Small-Sized Iron Oxide Nanoparticles for High-Resolution T_1 Magnetic Resonance Imaging Contrast Agents. *J. Am. Chem. Soc.* **2011**, *133*, 12624–12631.